The motion of a buoyant vortex filament

Ching Chang [1]† and Stefan G. Llewellyn Smith[1] [2]

[1]Department of Mechanical and Aerospace Engineering, Jacobs School of Engineering, UCSD, 9500 Gilman Drive, La Jolla, CA 92093-0411, USA

[2]Scripps Institution of Oceanography, UCSD, 9500 Gilman Drive, La Jolla, CA 92093-0213, USA

(Received xx; revised xx; accepted xx)

We investigate the motion of a thin vortex filament in the presence of buoyancy. The asymptotic model of Moore & Saffman (1972) is extended to take account of buoyancy forces in the force balance on a vortex element. The motion of a buoyant vortex is given by the transverse component of force balance, while the tangential component governs the dynamics of the structure in the core. We show that the local acceleration of axial flow is generated by the external pressure gradient due to gravity. The equations are then solved for vortex rings. An analytic solution for a buoyant vortex ring at a small initial inclination is obtained and it asymptotically agrees with literature.

Key words:

1. Introduction

Vortex dynamics forms an essential part of our understanding of fluid flows, especially for the most elusive flow phenomenon of turbulence (see Pullin & Saffman 1998). When vorticity is concentrated on a curve in space, the calculation of its self-induced motion is a challenging task. This is due to the singular nature of the Biot–Savart integral. A first approximation comes from the local induction approximation (LIA). For higher-order calculations, a cut-off method (see Saffman 1992, § 11) removes the neighborhood of the singularity when evaluating the integral. Rosenhead (1930) and Moore (1972) proposed adding a parameter to the denominator to desingularise the Biot-Savart kernel. Their method is equivalent to using a cutoff. Schwarz (1985) used a hybrid model combining a cut-off and the local induction approximation to calculate the motion of vortex filaments in superfluids. Callegari & Ting (1978) investigated vortex filaments with viscous cores and axial velocity using matched asymptotic expansions. More recently, Leonard (2010) calculated the motion of a thin vortex tube with an arbitrary core structure.

Vortex rings have also been intriguing entities in fluid flows, dating back to the pioneering work of Kelvin (1867). The theoretical speed of propagation for a thin ring with a hollow core was calculated by Hicks (1884). A good review of vortex rings can be found in Shariff *et al.* (1989). Vortex rings have been observed in geophysics and environmental fluid flows, e.g. bubble rings created by dolphins (see Marten *et al.* 1996) or a smoke ring from a fireball. The first investigation to take account of buoyancy for a vortex ring was the theoretical work and experiments of Turner (1957). Pedley (1968) performed a theoretical calculation for the motion of bubble rings with and without

† Email address for correspondence: chc054@eng.ucsd.edu

viscosity. Lundgren & Mansour (1991) computed the motion of bubble rings using a boundary integral method. The development of modern computational methods has led to the investigation of buoyant vortex rings, such as the 3D simulations of Cheng *et al.* (2013). In these studies, buoyant rings are allowed to evolve with their axis initially parallel to gravity, i.e. they start horizontally.

However, the motion of a general vortex filament in combination with buoyancy does not seem to have attracted theoretical interest previously. In this paper, we derive a mathematical model for the motion of a buoyant thin-core vortex filament. Buoyancy is incorporated by using a force balance on a vortex element. Equations of motion for a buoyant vortex filament of general shape are derived in the following section. Then the effect of buoyancy on the flow structure inside the core is discussed in section 3. In section 4, we use our model to investigate a special geometry, a buoyant vortex ring. An analytical solution for an initially non-horizontal ring with small inclination is obtained analytically. Its asymptotic form is compared with the solutions from the literature. In the final section, we draw conclusions and discuss possible future studies.

2. Mathematical Formulation

We use a force balance on a vortex filament to model its motion. The force balance argument is derived in Moore & Saffman (1972) (referred to as MS72 hereafter) for a constant density Euler flow. Here we consider different densities, ρ_1 and ρ_2, for the vortex filament itself and for the surrounding fluid respectively. Gravity is also included while it is omitted in MS72. The derivation in MS72 is an asymptotic analysis based on three approximations which we also follow: thin vortex core, $a\kappa \ll 1$, where a is the radius of the core and κ the curvature; slow time, $\partial/\partial t \approx \Gamma\kappa^2 \ln(1/a\kappa)$, where Γ is the circulation; and uniform core size, $\partial a/\partial s = O(a^2\kappa^2)$, where s is arclength.

In §2.1, we explain the idea of Moore and Saffman's momentum balance approach with examples when axial flow is zero. Then we extend their analysis to a buoyant vortex filament in §2.2.

2.1. *Momentum balance*

A vortex filament with thin core is considered while axial flow is neglected for now. According to the formulation in MS72, forces acting on an infinitesimal section of filament can be divided into two categories, $\mathbf{F}_E$ and $\mathbf{F}_I$, referred to exterior and interior forces respectively. The exterior force is the force per unit length exerted on the filament core boundary by the fluid outside, and is given by

$$\mathbf{F}_E = \Gamma\left(\mathbf{V}_E + \mathbf{V}_I - \frac{\partial \mathbf{R}}{\partial t}\right) \times \mathbf{t} + \frac{\Gamma^2}{4\pi}\kappa\mathbf{n}\left(\ln\frac{8}{a\kappa} - 1\right). \tag{2.1}$$

Here $\partial\mathbf{R}/\partial t$ is the local motion of the filament itself, $\mathbf{V}_E$ is the background flow evaluated at the filament centerline, and $\mathbf{V}_I$ is the velocity contributed by the rest of the filament. It accounts for the non-singular part of Biot-Savart law and can be evaluated using the desingularized Biot-Savart integral,

$$\mathbf{V}_I(\mathbf{R}_0) = \frac{\Gamma}{4\pi}\left[\int \frac{\mathrm{d}\mathbf{R} \times (\mathbf{R}_0 - \mathbf{R})}{|\mathbf{R}_0 - \mathbf{R}|^3} - \int \frac{\mathrm{d}\mathbf{R}_\odot \times (\mathbf{R}_0 - \mathbf{R}_\odot)}{|\mathbf{R}_0 - \mathbf{R}_\odot|^3}\right]. \tag{2.2}$$

The notation $\mathbf{R}_0$ in the second integral indicates that it is taken along the osculating circle to $\mathbf{R}$ at $\mathbf{R}_0$, the point at which $\mathbf{V}_I$ is being evaluated. The first term on the RHS of (2.1) is the Kutta-Joukowski lift on the filament. The last two terms are the effect of

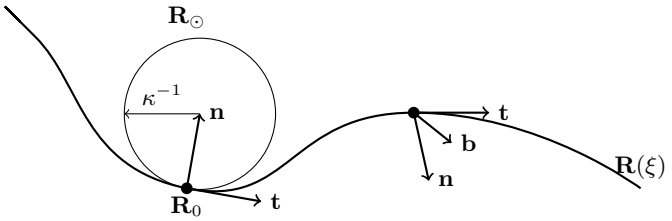

FIGURE 1. A filament $\mathbf{R}$ in space is parameterized by ξ. Its tangent, normal and binormal vectors are defined using the Frenet-Serret formulas. The osculating circle $\mathbf{R}_\odot$ associated with the point $\mathbf{R}_0$ has radius κ^{-1}.

pressure reduction on the core boundary due to the curvature of filament. The vectors $\mathbf{t}$, $\mathbf{n}$ are local unit tangent and normal vectors defined by

$$\mathbf{t} = \frac{\partial \mathbf{R}/\partial \xi}{|\partial \mathbf{R}/\partial \xi|}, \qquad \kappa \mathbf{n} = \frac{\partial \mathbf{t}}{\partial s}, \tag{2.3}$$

where ξ is an arbitrary parameterization of the curve $\mathbf{R}$ and s is arclength. The binormal vector is the cross product of tangent and normal vectors, $\mathbf{b} = \mathbf{t} \times \mathbf{n}$ (see figure 1).

The interior force comes from integrating the pressure over the end surface and then taking the derivative along the tangent of the filament. Due to the curvature, the net result is in the normal direction. This gives

$$\mathbf{F}_I = \pi \int_0^a r v(r)^2 \,\mathrm{d}r \kappa \mathbf{n} + \frac{\Gamma^2}{8\pi} \kappa \mathbf{n}, \tag{2.4}$$

where $v(r)$ is the azimuthal velocity within the core. The second term on the RHS matches the pressure reduction on the boundary from outside. This represents the force acting on the both ends of an infinitesimal filament. We have not included axial flow yet, so this is solely due to the pressure. Then the balance of forces, which is correct to $O(a^2\kappa^2)$ based on the assumptions at the beginning of § 2, gives

$$\mathbf{F}_E + \mathbf{F}_I = 0, \tag{2.5}$$

and the motion is determined by taking cross product of the force balance with the tangent $\mathbf{t}$,

$$\frac{\partial \mathbf{R}}{\partial t} = \mathbf{V}_E + \mathbf{V}_I + \frac{\Gamma}{4\pi} \kappa \mathbf{b} \left(\ln \frac{8}{a\kappa} - \frac{1}{2} + \frac{\mu}{4} \right), \tag{2.6}$$

with

$$\mu = \frac{1}{2} a^2 \overline{v^2} = \frac{16\pi^2}{\Gamma^2} \int_0^a r v(r)^2 \,\mathrm{d}r \tag{2.7}$$

and the bar denoting the average over the cross-section. For the motion of a vortex ring in a quiescent fluid, this gives

$$\frac{\partial \mathbf{R}}{\partial t} = \frac{\Gamma}{4\pi} \kappa \mathbf{b} \left(\ln \frac{8}{a\kappa} - \frac{1}{2} + \frac{\mu}{4} \right), \tag{2.8}$$

since $\mathbf{V}_I$ vanishes for rings. The parameter μ is determined by the flow structure inside the core. If the vorticity is uniform within the core, $\mu = 1$ while $\mu = 0$ for a hollow core. In the discussion so far, the density has been constant.

2.2. *Motion with buoyancy*

Now we consider density difference by setting the core density to ρ_1 and outside density to ρ_2. The exterior forces account for the forces acting on the boundary which forms the lateral surface of the element. In § 5 of MS72, the velocity on the boundary is first obtained by matching the asymptotic solutions from both sides. The flow is irrotational outside, so the potential and the boundary are expanded in κ

$$\phi = \phi_0 + \phi_1 + \phi_2 + \cdots, \qquad a = a_0 + a_1 + a_2 + \cdots. \tag{2.9}$$

Then the pressure is computed using Bernoulli's equation, (5.16) of MS72. The calculation for velocity is kinematic so we follow it. Adding gravity to Bernoulli's equation gives

$$p + \rho_2 \left[\frac{1}{2}(\boldsymbol{\nabla}\phi_0)^2 + \boldsymbol{\nabla}\phi_0 \cdot \boldsymbol{\nabla}\phi_1 - \frac{\partial \mathbf{R}}{\partial t} \cdot \boldsymbol{\nabla}\phi_0 + (z - Z)g \right] = 0, \tag{2.10}$$

where the local r-θ plane is perpendicular to $\mathbf{t}$ and $z = Z$ is the vertical position of the centerline (see figure 2). The leading-order potentials ϕ_0 is given in (5.8) of MS72 as

$$\phi_0 = \frac{\Gamma\theta}{2\pi}. \tag{2.11}$$

The first-order potential is then given in (5.15) of MS72 as

$$\begin{aligned}\phi_1 =& (\mathbf{V}_E + \mathbf{V}_I) \cdot (X\mathbf{n} + Y\mathbf{b}) - \frac{a_0^2}{r^2}\left(\frac{\partial \mathbf{R}}{\partial t} - \mathbf{V}_E - \mathbf{V}_I\right) \cdot (X\mathbf{n} + Y\mathbf{b}) + \frac{\Gamma Y}{4\pi}\kappa \ln\frac{8}{r\kappa} \\ &+ \frac{\Gamma Y a_0^2}{4\pi r^2}\kappa\left(\ln\frac{8}{a_0\kappa} - 1\right) + \int (\mathbf{V}_E + \mathbf{V}_I) \cdot \mathbf{t}\,\mathrm{d}s,\end{aligned} \tag{2.12}$$

where (X, Y) are coordinates on the **n**-**b** plane of the Frenet–Serret frame scaled by $O(\kappa^{-1})$ so that $\mathbf{x} = \mathbf{R} + X\mathbf{n} + Y\mathbf{b}$.

Therefore the pressure is given by (compare with 5.17 in MS72)

$$p = \rho_2 \left[-\frac{\Gamma^2}{8\pi^2 a^2} + \frac{\Gamma}{\pi a}\left(\frac{Y}{a}\mathbf{Q} \cdot \mathbf{n} - \frac{X}{a}\mathbf{Q} \cdot \mathbf{b}\right) - \frac{\Gamma^2 X}{4\pi^2 a^2}\kappa\left(\ln\frac{8}{a\kappa} - \frac{1}{2}\right)\right] + \rho_2(Z - z)g, \tag{2.13}$$

where $\mathbf{Q} = \mathbf{V}_E + \mathbf{V}_I - \partial\mathbf{R}/\partial t$ is the relative velocity between the surrounding fluid and the vortex filament. Integrating the pressure per unit length $\mathrm{d}s$ we obtain the exterior force,

$$\mathbf{F}_E = \rho_2 \left[\Gamma\mathbf{Q} \times \mathbf{t} + \frac{\Gamma^2}{4\pi}\left(\ln\frac{8}{a\kappa} - \frac{1}{2}\right)\kappa\mathbf{n} - \frac{\Gamma^2}{8\pi}\kappa\mathbf{n} + \pi a^2 g\mathbf{z}\right], \tag{2.14}$$

where $g\mathbf{z} = -\mathbf{g}$ and the last term is the weight of the surrounding fluid displaced by the filament, i.e. Archimedes' principle. Note that on the boundary $r = a$, as $X, Y \to 0$, the pressure becomes

$$p(r = a) = p_a = \rho_2 \left[-\frac{\Gamma^2}{8\pi^2 a^2} + (Z - z)g \right]. \tag{2.15}$$

This will be the boundary condition for the subsequent calculation of the interior forces.

MS72 starts its discussion of the interior forces by calculating the pressure acting on both ends of the segment. In MS72, the pressure is assumed to be symmetric about the centerline of the filament and calculated using (6.1) from MS72. Here we include density and gravity, yielding

$$\frac{\partial p}{\partial r} = \rho_1 \left(\frac{v_0^2}{r} + g_r \right), \tag{2.16}$$

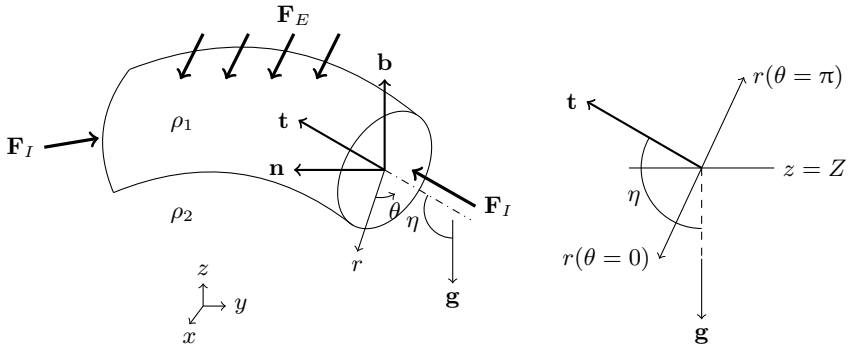

FIGURE 2. The coordinate system on a small element of the filament. The unit tangent $\mathbf{t}$ is perpendicular to the r-θ plane and its angle with the gravity is η. We define $\theta = 0$ when the angle between r and $\mathbf{g}$ is minimal.

where r is the local radial coordinate and v_0 is the azimuthal velocity in the interior. g_r is the projection of gravity on r. The pressure depends on r and θ while it depends only on r in MS72.

The force due to pressure acting on one end is

$$\begin{aligned} -\int_0^{2\pi}\int_0^a pr\,\mathrm{d}r\,\mathrm{d}\theta &= \frac{1}{2}\int_0^{2\pi}\left[\int_0^a r^2\frac{\partial p}{\partial r}\,\mathrm{d}r - a^2 p(r=a)\right]\mathrm{d}\theta \\ &= \frac{1}{2}\left(\rho_1\pi a^2\overline{v^2} + \int_0^{2\pi}\int_0^a r^2 g_r\,\mathrm{d}r\,\mathrm{d}\theta\right) + \rho_2\left(\frac{\Gamma^2}{8\pi} - \pi a^2 g s\cos\eta\right), \end{aligned} \tag{2.17}$$

where the bar indicates the average over the end surface area. The double integral vanishes since $g_r = r\cos\theta\; g\sin\eta$. The last two terms come from evaluating the pressure on $r = a$ and using the geometric relation $z - Z = -(r\cos\theta\sin\eta + s\cos\eta)$, which illustrated in figure 2. The pressure force on the end acting along the filament is calculated by differentiating (2.17) with respect to s,

$$\rho_1\frac{\partial}{\partial s}\left(\frac{1}{2}\pi a^2\overline{v^2}\mathbf{t}\right) + \rho_2\left(\frac{\Gamma^2}{8\pi}\kappa\mathbf{n} - \pi a^2 g\cos\eta\;\mathbf{t}\right). \tag{2.18}$$

When axial flow is nonzero, there are two additional contributions to the interior force $\mathbf{F}_I$: the tangential momentum flux across the two ends of the infinitesimal filament, and the rate of change of tangential momentum inside. The momentum flux across the ends is given by combining (6.4) and (6.5) of MS72,

$$-\rho_1\iint w\left(w\mathbf{t} + \mathbf{u}_\perp + \frac{\partial\mathbf{R}}{\partial t}\right)\mathrm{d}A = -\rho_1\left(\pi a^2\overline{w^2}\mathbf{t} + \frac{a^2\overline{w}\Gamma}{4}\kappa\mathbf{b} + \pi a^2\overline{w}\frac{\partial\mathbf{R}}{\partial t}\right), \tag{2.19}$$

where w is the axial flow and the bar means the average over the cross section. The momentum flux carried by the mean axial flow is decomposed into local tangential component, local perpendicular component ($\mathbf{u}_\perp$ on the r-θ plane) and the motion of the filament, which correspond to those three terms respectively. The rate of change of tangential momentum inside is given by MS72 (6.6),

$$-\rho_1\frac{\partial\xi}{\partial s}\frac{\partial}{\partial t}\left(\pi a^2\overline{w}\mathbf{t}\frac{\partial s}{\partial\xi}\right) = -\rho_1\left[\pi\frac{\partial}{\partial t}(a^2\overline{w}\mathbf{t}) + \pi a^2\overline{w}\mathbf{t}\frac{\partial}{\partial t}\left(\ln\frac{\partial s}{\partial\xi}\right)\right]. \tag{2.20}$$

We have a density ρ_1 for the filament, so the two equations above are multiplied by

ρ_1. Finally, we combine all the interior forces (2.18)–(2.20) and obtain

$$\begin{aligned}\mathbf{F}_I =&\rho_1\pi\frac{\partial}{\partial s}\left[\left(\frac{1}{2}a^2\overline{v^2}-a^2\overline{w^2}\right)\mathbf{t}-a^2\overline{w}\frac{\partial\mathbf{R}}{\partial t}-\frac{a^2\overline{w}\Gamma}{4\pi}\kappa\mathbf{b}\right]-\rho_2\pi a^2 g\cos\eta\ \mathbf{t}\\&-\rho_1\pi\left[\frac{\partial}{\partial t}(a^2\overline{w}\mathbf{t})+a^2\overline{w}\mathbf{t}\frac{\partial}{\partial t}\left(\ln\frac{\partial s}{\partial\xi}\right)\right]+\rho_2\frac{\Gamma^2}{8\pi}\kappa\mathbf{n}.\end{aligned}\tag{2.21}$$

We balance all the forces using

$$\mathbf{F}_E+\mathbf{F}_I+\mathbf{F}_B=0,\tag{2.22}$$

where $\mathbf{F}_B=\rho_1\pi a^2\mathbf{g}$ is the body force, i.e. the filament's weight. The transverse component of the force balance becomes

$$\begin{aligned}&\rho_2\left[\Gamma\mathbf{Q}\times\mathbf{t}+\frac{\Gamma^2}{4\pi}\left(\ln\frac{8}{a\kappa}-\frac{1}{2}\right)\kappa\mathbf{n}\right]+(\rho_2-\rho_1)\pi a^2 g\left[\mathbf{z}-(\mathbf{t}\cdot\mathbf{z})\mathbf{t}\right]\\&+\rho_1\pi\left(\frac{1}{2}a^2\overline{v^2}-a^2\overline{w^2}+\frac{a^2\overline{w}\Gamma}{4\pi}\tau\right)\kappa\mathbf{n}-\rho_1\left[2\pi a^2\overline{w}\frac{\partial\mathbf{t}}{\partial t}+\Gamma\frac{\partial}{\partial s}\left(\frac{a^2\overline{w}}{4}\kappa\right)\mathbf{b}\right]=0.\end{aligned}\tag{2.23}$$

Note that $\partial\mathbf{b}/\partial s=-\tau\mathbf{n}$ where τ is torsion. The $\mathbf{t}$-component is related to the core structure which will be discussed in the next section. The motion is given by taking the cross product of $\mathbf{t}$ with (2.23),

$$\begin{aligned}\frac{\partial\mathbf{R}}{\partial t}=&\mathbf{V}_E+\mathbf{V}_I+\frac{\Gamma}{4\pi}\kappa\mathbf{b}\left(\ln\frac{8}{a\kappa}-\frac{1}{2}+\frac{1}{4}\frac{\rho_1}{\rho_2}\right)+\left(1-\frac{\rho_1}{\rho_2}\right)\frac{\pi a^2 g}{\Gamma}\mathbf{t}\times\mathbf{z}\\&+\frac{\rho_1}{\rho_2}\left(-\frac{\pi a^2\overline{w^2}}{\Gamma}+\frac{a^2\overline{w}}{4}\tau\right)\kappa\mathbf{b}-\frac{\rho_1}{\rho_2}\left[\frac{2\pi a^2\overline{w}}{\Gamma}\mathbf{t}\times\frac{\partial\mathbf{t}}{\partial t}-\frac{\partial}{\partial s}\left(\frac{a^2\overline{w}}{4}\kappa\right)\mathbf{n}\right].\end{aligned}\tag{2.24}$$

To calculate the motion of a buoyant vortex filament using (2.24), one still needs the evolution equations for a and $\overline{w}$ which will be derived in the following section.

3. The internal structure

In order to calculate $\overline{w}$, we look into the flow structure within the core. This is achieved by examining the tangential component of (2.22):

$$\begin{aligned}&\rho_1\pi\frac{\partial}{\partial s}\left(\frac{1}{2}a^2\overline{v^2}-a^2\overline{w^2}\right)-2\rho_1\pi a^2\overline{w}\frac{\partial}{\partial t}\left(\ln\frac{\partial s}{\partial\xi}\right)-\rho_1\pi\left[V_{||}\frac{\partial}{\partial s}(a^2\overline{w})+\frac{\partial}{\partial t}(a^2\overline{w})\right]\\&=(\rho_2-\rho_1)\pi a^2 g\cos\eta\end{aligned}\tag{3.1}$$

where $V_{||}=\mathbf{t}\cdot\partial\mathbf{R}/\partial t$ is the tangential velocity. Buoyancy contributes an extra term when we compare (3.1) to (8.15) in MS72. To simplify the tangential equation, (8.5) in MS72, the decomposition $w=W(t)+q(s,t)+\Gamma\chi(r/a)/b$ is used, with a constant length b and with $\chi(r/a)$ the variation of w in the r-θ plane. This is justified based on the argument that q is $O(\kappa)$. We shall use

$$w=\overline{w}(s,t)+\frac{\Gamma}{b}\chi(\frac{r}{a})\tag{3.2}$$

for buoyant case here, since the dependence of w on s (and ξ) is $O(1)$ and $\overline{\chi}=0$. We then obtain

$$\overline{w^2}=\overline{w}^2(s,t)+\frac{\Gamma^2}{b^2}\nu\tag{3.3}$$

with a constant

$$\nu = 2\int_0^a \chi^2(\frac{r}{a})\ r\mathrm{d}r. \tag{3.4}$$

The continuity equation in (8.10) of MS72 for the vorticity core is

$$\frac{\partial\xi}{\partial s}\frac{\partial}{\partial t}\left(a^2\frac{\partial s}{\partial\xi}\right) + a^2\frac{\partial\overline{w}}{\partial s} = 0. \tag{3.5}$$

For incompressible flow, the volume of the core is conserved with a uniform core size so that

$$\frac{\mathrm{d}}{\mathrm{d}t}(a^2 L) = 0, \tag{3.6}$$

where $L(t)$ is the total length of the filament. It can be shown that using (3.5) and (3.6),

$$\frac{\partial\overline{w}}{\partial s} = -\frac{\partial}{\partial t}\left(\ln\frac{\partial s}{\partial\xi}\right) + \frac{1}{L}\frac{\mathrm{d}L}{\mathrm{d}t}, \tag{3.7}$$

which is identical to (8.12) in MS72. From (2.7) we find that $a^2\overline{v^2}$ is a constant with respect to s and (3.3) gives $\partial\overline{w^2}/\partial s = \partial\overline{w}^2/\partial s$. The tangential component then becomes

$$-\rho_1\pi\frac{D}{Dt}(L\overline{w}) = (\rho_2-\rho_1)\pi L g\cos\eta, \tag{3.8}$$

where $D/Dt = \partial/\partial t + V_{||}\partial/\partial s$ is defined to be the material derivative along the filament.

In general, the buoyancy force will accelerate or decelerate the axial flow inside the core. An exception is when the the tangent vector and gravity are perpendicular to each other, i.e. $\eta = \pi/2$; in this case $L\overline{w}$ is conserved. We will examine a nearly horizontal ring in this circumstance in the next section. It is worth noting that in the hollow vortex limit where $\rho_1 \to 0$, the equation becomes singular. This is due to our assumption of slow time which removes the small time scale and the large acceleration due to an adjustment to balance with the RHS of (3.8). The remedy should be reformulating the force balance and including the inertial term. However, such a treatment lies beyond the scope of this paper. For a buoyant vortex filament of a given shape $\mathbf{R}$, its motion can be calculated using (2.24) and (3.2) with a given density ratio, ρ_1/ρ_2. For the case of non-zero axial flow inside the core, an additional equation (3.8) is coupled with (2.24) and (3.6) to determine the motion of a buoyant vortex filament.

4. Solution for rings

We consider a vortex ring $\mathbf{R}$ of light fluid in a heavier ambient, centered at the origin with radius R_0 and its axis initially inclined at an angle α_0 from the direction of gravity (see Figure 3). The equation of motion (2.24) for the ring becomes

$$\begin{aligned}\frac{\partial\mathbf{R}}{\partial t} = \frac{\Gamma}{4\pi R}\mathbf{b}\left(\ln\frac{8R}{a} - \frac{1}{2} + \frac{1}{4}\frac{\rho_1}{\rho_2}\right) + \left(1-\frac{\rho_1}{\rho_2}\right)\frac{\pi a^2 g}{\Gamma}\mathbf{t}\times\mathbf{z} \\ + \frac{\rho_1}{\rho_2}\left[-\frac{\pi a^2\overline{w^2}}{\Gamma R}\mathbf{b} - \frac{2\pi a^2\overline{w}}{\Gamma}\mathbf{t}\times\frac{\partial\mathbf{t}}{\partial t} + \frac{a^2}{4R}\frac{\partial\overline{w}}{\partial s}\mathbf{n}\right].\end{aligned} \tag{4.1}$$

The ring radius R will vary in time, but the volume of the core is conserved for incompressible flow:

$$a^2 R = a_0^2\ R_0. \tag{4.2}$$

4.1. *Formulation*

We use local coordinates on the ring defined by

$$\mathbf{R}(t,\theta) = \mathbf{X}_c(t) + R(t) \begin{bmatrix} \cos\theta\cos\alpha(t) \\ \sin\theta \\ \cos\theta\sin\alpha(t) \end{bmatrix}, \tag{4.3}$$

whose time derivative is

$$\frac{\partial \mathbf{R}}{\partial t} = \frac{\mathrm{d}\mathbf{X}_c}{\mathrm{d}t} + \frac{\mathrm{d}R}{\mathrm{d}t} \begin{bmatrix} \cos\theta\cos\alpha \\ \sin\theta \\ \cos\theta\sin\alpha \end{bmatrix} + R\frac{\mathrm{d}\alpha}{\mathrm{d}t} \begin{bmatrix} -\cos\theta\sin\alpha \\ 0 \\ \cos\theta\cos\alpha \end{bmatrix}. \tag{4.4}$$

Using the Frenet–Serret formulas, we obtain

$$\mathbf{n} = \begin{bmatrix} -\cos\theta\cos\alpha \\ -\sin\theta \\ -\cos\theta\sin\alpha \end{bmatrix}, \quad \mathbf{b} = \begin{bmatrix} -\sin\alpha \\ 0 \\ \cos\alpha \end{bmatrix}, \quad \mathbf{t}\times\frac{\partial \mathbf{t}}{\partial t} = \mathbf{n}\frac{\mathrm{d}\alpha}{\mathrm{d}t}\sin\theta. \tag{4.5}$$

The equation of motion (4.1) becomes

$$\frac{\partial \mathbf{R}}{\partial t} = \frac{U+W_1}{R} \begin{bmatrix} -\sin\alpha \\ 0 \\ \cos\alpha \end{bmatrix} + \frac{\beta}{R} \begin{bmatrix} \cos\theta \\ \sin\theta\cos\alpha \\ 0 \end{bmatrix} + \frac{W_2}{R} \begin{bmatrix} -\cos\theta\cos\alpha \\ -\sin\theta \\ -\cos\theta\sin\alpha \end{bmatrix} \tag{4.6}$$

where

$$U(R) = \frac{\Gamma}{4\pi}\left(\frac{3}{2}\ln 4R - \frac{1}{2}\ln a_0^2 R_0 - \frac{1}{2} + \frac{1}{4}\frac{\rho_1}{\rho_2}\right), \quad \beta = \frac{\pi a_0^2 R_0}{\Gamma}\left(1 - \frac{\rho_1}{\rho_2}\right) g \tag{4.7}$$

come from vorticity and buoyancy, while

$$W_1(R) = -\frac{\rho_1}{\rho_2}\frac{\pi a_0^2 R_0 \overline{w^2}}{\Gamma R}, \quad W_2(R,\theta) = \frac{\rho_1}{\rho_2}\left(-\frac{2\pi a_0^2 R_0 \overline{w}}{\Gamma}\frac{\mathrm{d}\alpha}{\mathrm{d}t}\sin\theta + \frac{a_0^2 R_0}{4R}\frac{\partial \overline{w}}{\partial s}\right) \tag{4.8}$$

are associated with axial flow inside the core.

Combining (4.4) and (4.6), we obtain a set of evolution equations for $\mathbf{X}_c$:

$$\frac{\mathrm{d}x_c}{\mathrm{d}t} = -\frac{U+W_1}{R}\sin\alpha, \quad \frac{\mathrm{d}y_c}{\mathrm{d}t} = 0, \quad \frac{\mathrm{d}z_c}{\mathrm{d}t} = \frac{U+W_1}{R}\cos\alpha, \tag{4.9}$$

which is coupled to the evolution of R and α by

$$\frac{\mathrm{d}R}{\mathrm{d}t} = \frac{\beta}{R}\cos\alpha - \frac{W_2}{R}, \quad \frac{\mathrm{d}\alpha}{\mathrm{d}t} = -\frac{\beta}{R^2}\sin\alpha, \quad \frac{\mathrm{d}}{\mathrm{d}t}(R\sin\alpha) = -\frac{W_2}{R}\sin\alpha. \tag{4.10}$$

For a ring with density equal to the ambient value, there is no buoyancy, so that $\beta = 0$ and $\mathrm{d}\alpha/\mathrm{d}t = 0$. Then if the axial flow $\overline{w}$ is a constant then $W_2 = 0$ and W_1 is a constant. Therefore $\mathrm{d}R/\mathrm{d}t = 0$ and the ring radius remains constant. As we know, a vortex ring with no buoyancy just moves without expansion or turning. Axial flow changes its translation speed by $-\pi a^2\overline{w^2}/R\Gamma$.

When buoyancy is present, $\beta \neq 0$. Axial flow is locally accelerated due to the pressure gradient discussed in section 3. In this case, $\overline{w}$ has temporal and spatial dependence, and $\mathrm{d}R/\mathrm{d}t$ varies with θ. As a result, the ring cannot maintain its circular shape and (4.3) becomes invalid. On the other hand, if axial flow is always negligible, an analytic solution for (4.9) and (4.10) can be derived. We may take the ring to be nearly horizontal, so that $\cos\eta \approx 0$ and (3.8) gives the solution $\overline{w} \approx 0$. Then we may solve the evolution equations analytically.

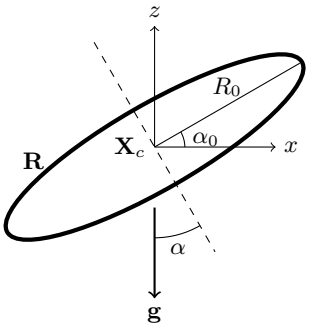

FIGURE 3. Initial setting of a vortex ring is tilting an angle α_0 from x axis. Gravity $\mathbf{g}$ is in the negative z direction.

4.2. *A slightly non-horizontal buoyant ring*

According to Turner (1957) and Pedley (1968), we know that the radius of a horizontal ring grows as it rises. We also anticipate that α will decrease, so that the ring will turn toward the horizontal. Here we take the initial angle α_0 to be small, and require no axial flow so that $W_1 = W_2 = 0$ while keeping the buoyancy term. The evolution equations become

$$\frac{\mathrm{d}x_c}{\mathrm{d}t} = -\frac{U}{R}\sin\alpha, \quad \frac{\mathrm{d}y_c}{\mathrm{d}t} = 0, \quad \frac{\mathrm{d}z_c}{\mathrm{d}t} = \frac{U}{R}\cos\alpha, \tag{4.11}$$

$$\frac{\mathrm{d}R}{\mathrm{d}t} = \frac{\beta}{R}\cos\alpha, \quad \frac{\mathrm{d}\alpha}{\mathrm{d}t} = -\frac{\beta}{R^2}\sin\alpha, \quad \frac{\mathrm{d}}{\mathrm{d}t}(R\sin\alpha) = 0. \tag{4.12}$$

The last equation gives $R\sin\alpha = R_0\sin\alpha_0$. Then we solve for α by integrating (4.12b) to obtain

$$\int^{\alpha} \frac{\mathrm{d}\alpha'}{\sin^3\alpha'} = -\frac{\beta t}{R_0^2\sin^2\alpha_0} + C_1.$$

The integral on the left hand side can be evaluated using the initial condition $\alpha(t=0) = \alpha_0$, giving

$$\frac{\beta t}{R_0^2\sin^2\alpha_0} = \frac{1}{2}\left(\csc\alpha\cot\alpha - \csc\alpha_0\cot\alpha_0 + \ln\frac{\csc\alpha_0 - \cot\alpha_0}{\csc\alpha - \cot\alpha}\right). \tag{4.13}$$

Since α is an implicit function of time, we will also solve other quantities implicitly in terms of α rather than explicitly in time. The radius is found by integrating (4.12a), yielding

$$\frac{1}{2}\mathrm{d}R^2 = \beta\cos\alpha\frac{\mathrm{d}t}{\mathrm{d}\alpha}\mathrm{d}\alpha. \tag{4.14}$$

With $R(\alpha_0) = R_0$, the solution is

$$R(\alpha) = R_0\frac{\sin\alpha_0}{\sin\alpha}. \tag{4.15}$$

It is trivial to conclude that $y_c(t) = 0$. Integrating the equations for $x_c(t)$, $z_c(t)$ with initial condition $(0, 0)$ yields

$$x_c(t) = \frac{\Gamma}{4\pi}R_0\sin\alpha_0\left[A_0\left(\ln\frac{\csc\alpha - \cot\alpha}{\csc\alpha_0 - \cot\alpha_0}\right) - \frac{3}{2}\int_{\alpha_0}^{\alpha}\frac{\ln(\sin\alpha')}{\sin\alpha'}d\alpha'\right] \tag{4.16}$$

and

$$z_c(t) = \frac{\Gamma}{4\pi} R_0 \sin\alpha_0 \left\{ A_0(\csc\alpha - \csc\alpha_0) - \frac{3}{2}\left[\frac{\ln(\sin\alpha)+1}{\sin\alpha} - \frac{\ln(\sin\alpha_0)+1}{\sin\alpha_0} \right] \right\}, \quad (4.17)$$

where

$$A_0 = \frac{3}{2}\ln(R_0\sin\alpha_0) + \ln\frac{8}{a_0\sqrt{R_0}} - \frac{1}{2} + \frac{1}{4}\frac{\rho_1}{\rho_2}$$

is a constant determined by the initial condition. The integral in x_c is related to the dilogarithm function Li_2 and is given by

$$\begin{aligned}\int_{\alpha_0}^{\alpha} \frac{\ln(\sin\alpha')}{\sin\alpha'}\mathrm{d}\alpha' = & -\frac{1}{4}\ln 2\left[\ln\frac{1+\cos\alpha}{1-\cos\alpha} - \ln\frac{1+\cos\alpha_0}{1-\cos\alpha_0}\right] \\ & + \frac{1}{8}\left[\ln^2(1-\cos\alpha) - \ln^2(1+\cos\alpha) - \ln^2(1-\cos\alpha_0) + \ln^2(1+\cos\alpha_0)\right] \\ & + \frac{1}{4}\left[Li_2(\frac{1+\cos\alpha}{2}) - Li_2(\frac{1-\cos\alpha}{2}) - Li_2(\frac{1+\cos\alpha_0}{2}) + Li_2(\frac{1-\cos\alpha_0}{2})\right]. \end{aligned} \quad (4.18)$$

4.3. *The limit $\alpha \to 0$ as $t \to \infty$*

Using the small angle expansion, we approximate

$$\frac{\beta t}{R_0^2 \sin^2\alpha_0} = \frac{1}{2}\left(\alpha^{-2} - \ln\frac{\alpha}{2}\right) + O(1), \quad (4.19)$$

so that, to leading order,

$$\alpha(t) \approx \frac{R_0\sin\alpha_0}{\sqrt{2\beta t}}. \quad (4.20)$$

Therefore, we need $\alpha \to 0$ as $t \to \infty$. The ring turns to the horizontal for long times.

The radius is approximately

$$R(t) = R_0\frac{\sin\alpha_0}{\sin\alpha(t)} \approx \sqrt{2\beta t}. \quad (4.21)$$

This asymptotic behavior agrees with the investigations by Turner (1957) and Lundgren & Mansour (1991).

The trajectory is approximately

$$x_c \approx -\frac{3\Gamma}{64\pi} R_0\sin\alpha_0\left[(\ln t)^2 + \frac{8}{3}A_0\ln t\right]; \quad z_c \approx \frac{3\Gamma}{16\pi}\sqrt{2\beta}\; t^{\frac{1}{2}}\ln t, \quad (4.22)$$

where x_c should be asymptotically a constant as $t \to \infty$. If we differentiate z_c with respect to time, we find

$$\frac{\mathrm{d}z_c}{\mathrm{d}t} \approx \frac{3\Gamma}{16\pi}\sqrt{2\beta}\; t^{-\frac{1}{2}}\left(\frac{1}{2}\ln t + 1\right). \quad (4.23)$$

This agrees with Pedley's result of the speed varying as $t^{-1/2}\ln t$ for a horizontal ring.

5. Conclusion

We have studied the motion of a buoyant vortex filament using a force balance approach, to take account for all the forces acting on a element of vortex whose density is different from its surrounding fluid. Buoyancy forces arise from integrating pressure

over the boundary. For a simple geometry such as a ring, buoyancy causes its radius to increase when it moves against gravity; conversely a buoyant ring moving downward will shrink. The motion of a buoyant filament also depends on axial flow inside its core. An investigation of the internal structure shows that axial flow is generated inside the core, and its rate of change is proportional to the projection of gravity on the local tangent. The acceleration/deceleration of axial flow reaches maximum when the background pressure gradient aligns with the local tangent. If the tangent vector is horizontal, there is locally no acceleration of axial flow.

A set of equations (2.24), (3.6) and (3.8) are obtained for the motion of a buoyant vortex filament. For a filament of arbitrary shape, the calculation needs to be carried out numerically. For a simple circular geometry, we obtain an exact solution for the evolution of an initially non-horizontal ring, valid when the ring has small inclination so that axial flow is not significant. Our calculation shows that buoyancy will change the orientation of the ring and turn it to the horizontal. Our asymptotic solution agree with the results of Turner (1957) and Pedley (1968).

The solution for a ring given here is restricted by several assumptions. It is worth investigating when the angle α becomes large. In this case, it is also important to examine the effect of axial flow which becomes non-trivial and a numerical calculation is required. The other extension is to investigate a buoyant vortex ring with large core radius using axisymmetric contour dynamics. The stability analysis on a buoyant vortex ring is another intriguing topic.

This work was supported by NSF award CBET-1706934. C.C. acknowledges the Government Scholarship to Study Abroad from the Ministry of Education, Taiwan.

REFERENCES

Callegari, A.J. & Ting, L. 1978 Motion of a curved vortex filament with decaying vortical core and axial velocity. *SIAM J. Appl. Math.* **35**, 148–174.

Cheng, M., Lou, J. & Lim, T.T. 2013 Motion of a bubble ring in a viscous fluid. *Phys. Fluids* **25**, 067104.

Hicks, W. M. 1884 On the steady motion and small vibrations of a hollow vortex. *Phil. Trans. R. Soci. Lond.* A **175**, 161–195.

Kelvin, Lord 1867 The translatory velocity of a circular vortex ring. *Phil. Mag.* **33**, 511–512.

Leonard, A. 2010 On the motion of thin vortex tube. *Theor. Comput. Fluid Dyn.* **24**, 369–375.

Lundgren, T. S. & Mansour, N. N. 1991 Vortex ring bubbles. *J. Fluid Mech.* **224**, 177–196.

Marten, K., Shariff, K., Psarakos, S. & White, D.J. 1996 Ring bubbles of dolphins. *Sci. Am.* **275**, 82–87.

Moore, D.W. 1972 Finite amplitude waves on aircraft trailing vortices. *Aero. Quarterly* **23**, 307–314.

Moore, D. W. & Saffman, P. G. 1972 The motion of a vortex filament with axial flow. *Phil. Trans. R. Soci. Lond.* A **272**, 403–429.

Pedley, T.J. 1968 The toroidal bubble. *J. Fluid Mech.* **32**, 97–112.

Pullin, D. I. & Saffman, P. G. 1998 Vortex dynamics in turbulence. *Annu. Rev. Fluid Mech.* **30**, 31–51.

Rosenhead, L. 1930 The spread of vorticity in the wake behind a cylinder. *Proc. Roy. Soc.* A **127**, 590–612.

Saffman, P. G. 1992 *Vortex Dynamics*. Cambridge University Press.

Schwarz, K.W. 1985 Three-dimensional vortex dynamics in superfluid He: Line-line and line-boundary interactions. *Phys. Rev.* B **31**, 5782–5804.

Shariff, K., Leonard, A. & Ferziger, J. 1989 Dynamics of a class of vortex rings. *Tech. Rep.* 102257. NASA.

Turner, J.S. 1957 Buoyant vortex rings. *Proc. R. Soc. Lond.* A **239**, 61–75.